Chemical Science

ROYAL SOCIETY OF CHEMISTRY

EDGE ARTICLE

View Article Online
View Journal | View Issue

Cite this: *Chem. Sci.*, 2022, **13**, 439

All publication charges for this article have been paid for by the Royal Society of Chemistry

Ga^+-catalyzed hydrosilylation? About the surprising system $Ga^+/HSiR_3$/olefin, proof of oxidation with subvalent Ga^+ and silylium catalysis with perfluoroalkoxyaluminate anions†‡

Antoine Barthélemy, Kim Glootz, Harald Scherer, Annaleah Hanske and Ingo Krossing *

Already 1 mol% of subvalent $[Ga(PhF)_2]^+[pf]^-$ ($[pf]^- = [Al(OR^F)_4]^-$, $R^F = C(CF_3)_3$) initiates the hydrosilylation of olefinic double bonds under mild conditions. Reactions with $HSiMe_3$ and $HSiEt_3$ as substrates efficiently yield *anti*-Markovnikov and *anti*-addition products, while bulkier substrates such as HSi^iPr_3 are less reactive. Investigating the underlying mechanism by gas chromatography and STEM analysis, we unexpectedly found that H_2 and metallic Ga^0 formed. Without the addition of olefins, the formation of $R_3Si–F–Al(OR^F)_3$ (R = alkyl), a typical degradation product of the $[pf]^-$ anion in the presence of a small silylium ion, was observed. Electrochemical analysis revealed a surprisingly high oxidation potential of univalent $[Ga(PhF)_2]^+[pf]^-$ in weakly coordinating, but polar *ortho*-difluorobenzene of $E_{1/2}(Ga^+/Ga^0$; oDFB) = +0.26–0.37 V *vs.* Fc^+/Fc (depending on the scan rate). Apparently, subvalent Ga^+, mainly known as a reductant, initially oxidizes the silane and generates a highly electrophilic, silane-supported, silylium ion representing the actual catalyst. Consequently, the $[Ga(PhF)_2]^+[pf]^-/HSiEt_3$ system also hydrodefluorinates $C(sp^3)–F$ bonds in 1-fluoroadamantane, 1-fluorobutane and $PhCF_3$ at room temperature. In addition, both catalytic reactions may be initiated using only 0.2 mol% of $[Ph_3C]^+[pf]^-$ as a silylium ion-generating initiator. These results indicate that silylium ion catalysis is possible with the straightforward accessible weakly coordinating $[pf]^-$ anion. Apparently, the kinetics of hydrosilylation and hydrodefluorination are faster than that of anion degradation under ambient conditions. These findings open up new windows for main group catalysis.

Received 19th August 2021
Accepted 21st November 2021

DOI: 10.1039/d1sc05331k

rsc.li/chemical-science

Introduction

Classical Ga^I-sources, *e.g.* "GaI",[1,2] $Ga[GaX_4]$ (X = Cl, Br, and I)[3] or $GaCp^{(*)}$[4] do have some drawbacks in their applications: they undergo facile dis- or comproportionation reactions upon addition of σ-donating ligands,[1,5,6] due to the presence of reactive and strongly coordinating counterions such as $[GaX_4]^-$ [7] or, for Green's "GaI", have a non-homogenous composition[1,8] that hampered systematic studies of Ga^I chemistry for a long time. Subsequently, well-defined Ga^I compounds including $Ga^I[^{Dipp}NacNac]$ ($[^{Dipp}NacNac]^-$ = [(Dipp)NC(Me)CHC(Me)N(Dipp)]$^-$; Dipp = 2,6-diisopropylphenyl)[9] or $Ga^I[\{(Dipp)N{=}CH\}_2]$[10] allowed to investigate the interesting carbene-like reactivity of Ga^I (*vide infra*). Yet, they are no source for "naked" cationic Ga^+ to be tested in any application.

In this respect, the introduction of weakly coordinating anions (WCAs),[11,12] for example, in $[Ga_2Cp^*][B(Ar^F)_4]$[13] (Ar^F = 3,5-$(CF_3)_2C_6H_3$) and $[In_2Cp^*][B(C_6F_5)_4]$[14] was another improvement in subvalent M^I chemistry. However, the follow-up chemistry of these salts is complicated and the atom efficiency is limited because one excess equivalent of M(Cp*) (M = Ga or In) is released per M^+ ion introduced. Therefore, employing the $[pf]^-$ anion ($[pf]^- = [Al(OR^F)_4]^-$; $R^F = C(CF_3)_3$) in conjunction with weakly coordinating solvents now allows for the rational application of "naked" univalent gallium ions with the well-defined Ga^+ source $[Ga(PhF)_2][pf]$.[15,16] The respective indium salt $[In(PhF)_2][pf]$ was reported shortly thereafter.[17,18] Both are suitable for coordination chemistry with classical σ-donor ligands.[6] In addition, Wehmschulte has recently presented salts of the type $[Ga(arene)_x]A$ with $A = [CHB_{11}Cl_{11}]^-$ or $[B(C_6F_5)_4]^-$.[19] Still, these carborate or borate salts are expensive

Institut für Anorganische und Analytische Chemie, Freiburger Materialforschungszentrum (FMF), Universität Freiburg, Albertstr. 21, 79104 Freiburg, Germany. E-mail: krossing@uni-freiburg.de

† Dedicated to the occasion of the 60th birthday of Holger Braunschweig.

‡ Electronic supplementary information (ESI) available: Full experimental details, 1D- and 2D NMR spectra of the reactions are deposited. Details to the quantum chemical calculations are given together with the results of gas chromatographic, cyclic voltammetry, STEM/EDX measurements and crystallographic details. CCDC deposition number 2024333 (for $Et_3Si–F–Al[OC(CF_3)_3]_3$). For ESI and crystallographic data in CIF or other electronic format see DOI: 10.1039/d1sc05331k

and also difficult to synthesize, unlike the straightforward large-scale accessible $[pf]^-$ salts.[20]

Consequently, salts of the type $[M(arene)_x][pf]$ (M = Ga or In; $x = 1$–3) are increasingly employed as M^+ sources in catalysis, for example, in C–C bond forming reactions, like hydroarylation, hydrogenative cyclization, alkene transfer hydrogenation or Friedel–Crafts reactions.[21,22] Intriguingly, the univalent M^I salts display equal or even superior activity to more traditional M^{III} compounds.[22,23] In these reactions, the univalent metal ions presumably act as π-Lewis acids and coordinate to a CC double or triple bond. Confirming this hypothesis, recently the isolation of $[Ga(1,5\text{-COD})_2]^+[pf]^-$ (1,5-COD = 1,5-cyclooctadiene) as the first homoleptic main group metal olefin complex was reported.[24]

Moreover, our group has previously shown that univalent gallium catalyzes the polymerization of isobutylene.[25,26] DFT studies suggest that the reaction proceeds *via* oxidative addition of Ga^I, β-hydrides elimination and insertion of isobutylene units into the C–Ga bond. Chain growth could be terminated *via* reductive elimination from Ga^{III}, thereby regenerating catalytically active Ga^I.[25] Remarkably, the proposed reaction sequence is reminiscent of a coordinative polymerization mechanism, typically invoked for transition metals. In fact, spontaneous reductive H_2 elimination has been reported for cationic $[H_2Ga^{III}(PhF)_2]^+[CHB_{11}Cl_{11}]^-$, giving $[Ga^I(PhF)_2]^+[CHB_{11}Cl_{11}]^-$.[19] Additionally, it is well known that neutral and anionic Ga^I complexes readily add oxidatively to a variety of covalent element–element bonds of like and dislike elements, *e.g.* H–H,[27] H–C,[28] H–N,[27] H–O,[27] H–P,[27] H–Sn,[27] C–Cl [29] and group 15 and 16 element E–E bonds,[30] *inter alia*.[31,32] Only recently, a PPh_3-supported cationic Ga complex has been reported to insert into a H–P bond of a phosphonium cation.[124]

Such transition metal- or silylene-like[33] reactivity of univalent Ga^I results from the $4s^24p^0$ electron configuration[18] that potentially allows for oxidative addition and reductive elimination reactions in catalytic cycles. This encouraged us to investigate the catalytic potential of Ga^+ in other usually transition metal-catalyzed reactions. In this paper, we present a systematic investigation of the $[Ga(PhF)_2][pf]$-initiated hydrosilylation of olefinic double bonds, with a focus on mechanistic considerations. While working on this and independently of us, Wehmschulte reported that similarly the use of catalytic amounts of Ga^+ salts with the WCAs $[CHB_{11}Cl_{11}]^-$ or $[B(C_6F_5)_4]^-$ initiates hydrosilylation of 1-hexene and benzophenone.[19] Yet, no mechanistic investigations were performed and the authors refrained from speculations.

Hydrosilylation of C=C double bonds is an important Si–C bond forming reaction. It is widely used in industrial processes for the production of consumer goods, *e.g.* for the synthesis of silicone elastomers, resins or oils.[34–38] Although addition of a H–Si bond across C=C double bonds is exothermic by *ca.* 160 kJ mol^{-1}, the reaction is kinetically hindered. Thus, suitable catalytic systems are required, with first reports dating back to 1947, using a radical initiator.[39] The introduction of hexachloroplatinic acid $[H_2PtCl_6]\cdot H_2O$ (Speier's catalyst)[40] and, even more importantly, Karstedt's catalyst,[41] a dinuclear Pt(0) complex containing unsaturated disiloxanes, is an important milestone in homogeneous catalysis. Today, complexes containing precious transition metals such as rhodium,[42] iridium[43] and especially platinum are most commonly employed as catalysts, but Karstedt's catalyst still serves as the benchmark system.[35,36,38]

Nevertheless, Pt-catalyzed hydrosilylation reactions also suffer from drawbacks, since they are often accompanied by side reactions such as olefin-oligomerization, -hydrogenation and -isomerization, resulting in yield loss.[35] In some cases, the low selectivity of Pt-catalyzed hydrosilylation, as well as the high cost, insecurity of supply and environmental issues of platinum necessitate the search for alternative catalytic systems.[34,36,44]

Through extensive research in this field, it was found that hydrosilylation of multiple bonds can also be catalyzed by alkaline or alkaline earth metals,[45] lanthanides[46] and non-precious transition metals.[36,47] Besides this, group 13-based Lewis acids such as boranes as well as neutral and cationic Al^{III} compounds were shown to efficiently catalyze hydrosilylation reactions of olefins,[48–50] imines[51–54] or carbonyl compounds.[52,53,55–59] According to the Piers–Oestreich mechanism, the Lewis acid forms an adduct with the silane, thus polarizing the Si–H bond, increasing the electrophilicity of the silicon atom and facilitating the nucleophilic attack of the multiple bond.[49,56,58,60,61] For the aluminum halide-catalyzed hydrosilylation of alkynes, a different mechanism was proposed, with the aluminum halide coordinating to the multiple bond.[62] Only very few examples of Ga^{III} catalysts in hydrosilylation reactions have been reported in the literature.[44,63] They exclusively describe the hydrosilylation of carbonyl compounds[64] or CO_2.[65] To the best of our knowledge, the Ga^+ carborate and borate salts presented by Wehmschulte are the only gallium-based systems that have been employed to promote hydrosilylation of olefins so far, yet without any mechanistic investigation.[19]

Results and discussion

First, we turn to an overview of the hydrosilylation capacity of the $[Ga(PhF)_2][pf]$/silane/olefin system, before turning to mechanistic issues and further experimental and theoretical studies to understand the mechanism of the reaction.

Scope of the hydrosilylation reactions with $[Ga(PhF)_2][pf]$

The scope of the hydrosilylation reaction was investigated by employing $[Ga(PhF)_2][pf]$ (**1**) as the Ga^+ catalyst and using different organohydrosilanes H_xSiR_{4-x} (R = aryl or alkyl substituents) and olefin substrates, listed in Table 1. Reactions were carried out in *ortho*-difluorobenzene (*o*DFB) as NMR tube reactions. The yield was determined by NMR spectroscopy and was referred to the minimum substrate. Exemplary NMR spectra for all reactions as well as a detailed evaluation of NMR data are deposited in the ESI.‡

Changing the $[Ga(PhF)_2][pf]$ concentration. For the $HSiMe_3$/1-hexene system, the influence of the loading of **1** on the reaction kinetics was systematically investigated (Fig. 1, entries 1–3 in Table 1).

Table 1 Hydrosilylation reactions carried out in *o*DFB with $[Ga(PhF)_2][pf]$ (**1**) and the silane/olefin indicated. The yield of the main products as determined by NMR spectroscopy is given

#	Silane	Olefin	Molar ratio silane : olefin : **1**	*c* (olefin) [M]	Reaction time (temperature)	Main products	Yield[a]
1	$HSiMe_3$	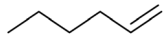	1.2 : 1.0 : 0.1	0.11	4 h (rt[b])	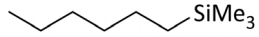	93%
2	$HSiMe_3$	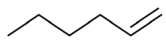	1.2 : 1.0 : 0.01	0.11	3 d (rt)	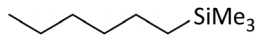	91%
3	$HSiMe_3$	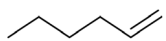	1.0 : 1.0 : 0.005	0.11	4.5 d (rt)	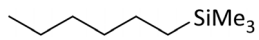	20%
4	$HSiMe_3$	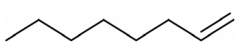	1.0 : 1.0 : 0.14	0.18	3 h (rt)	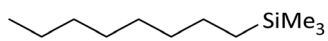	>97%
5	$HSiMe_3$		1.0 : 1.0 : 0.1	0.22	10 h (rt)	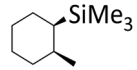	93%
6	$HSiMe_3$		1.0 : 1.0 : 0.05	0.11	1 d (rt)	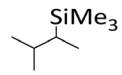	95%
7	$HSiMe_3$	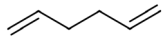	2.2 : 1.0 : 0.1	0.20	10 h (rt)	Crude mixture of products; olefin oligomerization and addition of scrambling products	—
8	$HSiMe_2Et$	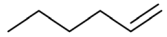	0.4 : 1.0 : 0.1	0.25	8 h (rt)	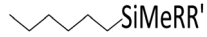 + oligomerized species	R = Me, R′ = Et: 38% R = Me, R′ = Me: 1% R = Et, R′ = Et: 2%; *ca.* 60% olefin oligomers 100% of silane consumed
9	$HSiMe_2Et$	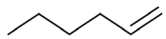	1.0 : 1.0 : 0.01	0.11	3.5 d (rt) + 9 h (60 °C)	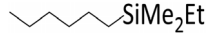	84%
10	$HSiMe_2Et$	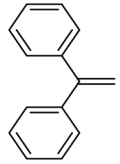	4.7 : 1.0 : 0.02	0.17	8 h (rt)	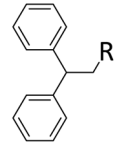	R = SiHMeEt: 48% R = $SiMe_2Et$: 31%; R = H: 6%; R = $SiHMe_2$: 5%; traces of other addition products and silane scrambling products; 100% of olefin consumed
11	$HSiMe_2Et$	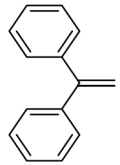	0.9 : 1.0 : 0.01	0.10	2 h (rt) + 1 d (60 °C)	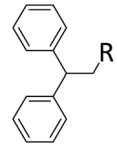	R = SiHMeEt: 74% R = H: 4%; and silane scrambling products like Me_3SiEt (7%)
12	$HSiEt_3$	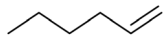	1.1 : 1.0 : 0.1	0.11	4 d (rt) + 1 d (60 °C)	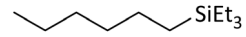	>97%
13	$HSiEt_3$	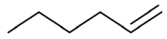	1.0 : 1.0 : 0.05	0.11	3.5 d (60 °C)	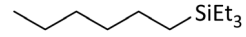	91%

Table 1 (*Contd.*)

#	Silane	Olefin	Molar ratio silane : olefin : **1**	*c* (olefin) [M]	Reaction time (temperature)	Main products	Yield[a]
14	$HSiEt_3$	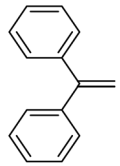	4.2 : 1.0 : 0.02	0.17	6 d (rt) + 4 h (60 °C)	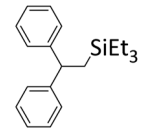	94%
15	$HSiEt_3$	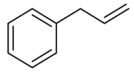	0.9 : 1.0 : 0.1	0.65	7 d (rt) + 2.5 d (60 °C)	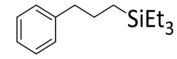	89%
16	$HSiEt_3$		0.8 : 1.0 : 0.05	0.11	7 d (60 °C) + 2.5 d (80 °C)	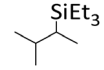	86%
17	$HSiEt_3$	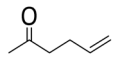	0.9 : 1.0 : 0.1	0.61	5 h (rt)	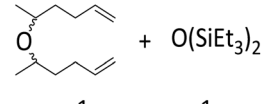 1 : 1	>90%[c]
18	HSi^iPr_3	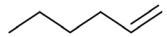	1.8 : 1.0 : 0.1	0.24	11 d (rt) + 2 d (60 °C)	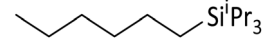	57%
19		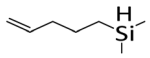	1.0 : 0.1	1.3	1 d (rt)		96%

[a] Determined by ^1H NMR spectroscopy, referred to the deficit substrate. [b] rt = room temperature. [c] 2,5-Dimethyltetrahydrofuran (7%) formed as a side product.

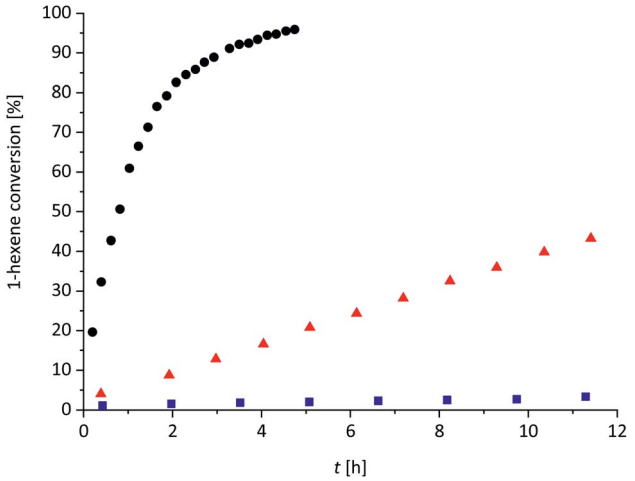

Fig. 1 Plot of 1-hexene conversion *versus* time for the catalytic hydrosilylation reaction of 1-hexene with 1.2 eq. Me_3SiH and 10 mol% **1** (black dots), with 1.2 eq. Me_3SiH and 1 mol% **1** (red triangles) and with 1.0 eq. Me_3SiH and 0.5 mol% **1** (blue squares) in *o*DFB (0.11 M for 1-hexene) at rt. The 1-hexene conversion was obtained by ^1H NMR integration (1-hexene conversion = *c* ($RH_2C–H_2C–SiMe_3$)/*c* ($RH_2C–H_2C–SiMe_3$ + $H_2C{=}CH–R$); R = ^{n}Bu).

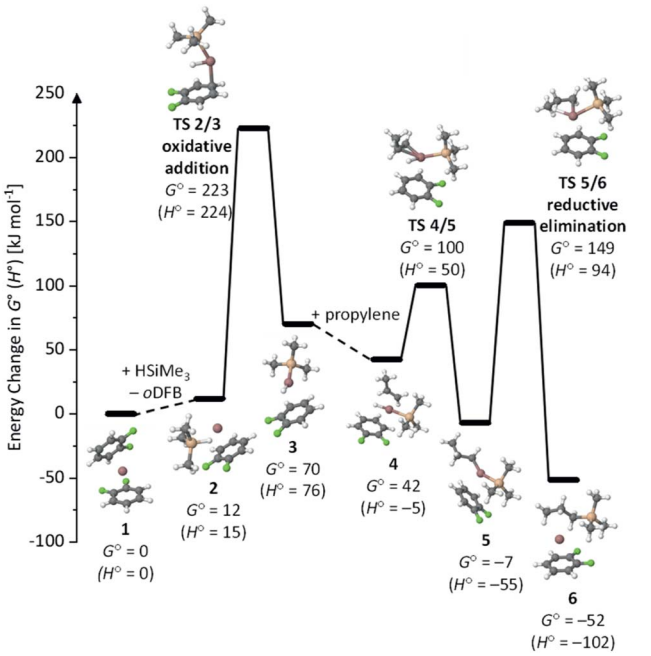

Scheme 1 Energy landscape for Ga^+-catalyzed hydrosilylation of propylene with $HSiMe_3$, according to a Ga^+-centered Chalk–Harrod mechanism (calculated at the RI-BP86(D3BJ)/def2-TZVPP level of theory; all values are expressed in kJ mol^{-1}).

Obviously, the use of 10 mol% **1** allows for fast hydrosilylation and loadings of 1% or lower slow down the reaction, but still initiate hydrosilylation of the olefin at room temperature.

Varying R in $HSiR_3$. The reactions with $HSiMe_3$ proceed smoothly at room temperature, even with trisubstituted olefins (entries 5 and 6), and selectively yield the *anti*-Markovnikov addition product.

With excess $HSiMe_2Et$, pronounced scrambling of the alkyl ligands is observed and the reaction with this silane is somewhat unselective (compare entries 10 and 14). In order to suppress these side reactions, $HSiMe_2Et$ and the olefin have to be mixed in a 1 : 1 stoichiometry. Probably, scrambling takes place with $HSiMe_3$ and $HSiEt_3$ as well. Yet, these silanes are more symmetrical and have only two different ligands, so that ligand scrambling is less pronounced in the addition product. However, if excess $HSiMe_3$ is employed, the hydrosilane reacts with the hydrosilylation product $RSiMe_3$ under formation of $SiMe_4$ and $RSiMe_2H$ after completion of hydrosilylation. Obviously, ligand redistribution competes with the hydrosilylation reaction. Oligomerization of the olefin (entry 8) is another typical side reaction, especially when excess olefin is applied. The reactions with $HSiEt_3$ usually require heating at 60 °C for several hours or days; a similar observation was reported by Wehmschulte.[19] However, the hydrosilylation of trisubstituted olefins with $HSiEt_3$ is complicated and rather slow (entry 16). The addition of bulkier HSi^iPr_3 is considerably slower than the reaction with less sterically hindered silanes, even with 1-hexene (entry 18).

Phenylsilanes H_3SiPh and H_2SiPh_2 are no suitable substrates. With these silanes, extensive ligand redistribution under formation of silanes such as $H–SiH_3$ and $H–SiPh_3$ takes place, as well as the addition of these silanes (Section 2.1.11 in ESI‡). Obviously, ligand scrambling is faster than hydrosilylation for phenylsilanes.

Varying the olefin. The hydrosilylation of monosubstituted (*e.g.* 1-hexene), disubstituted (1,1-diphenylethylene) and trisubstituted (1-methylcyclohexene) olefins is possible with the $HSiR_3$/**1** system. Intramolecular hydrosilylation can also be performed (entry 19). However, in an unsaturated carbonyl compound, the C=C double bond does not react and instead formation of a symmetrical ether and a disiloxane is observed (entry 17). Similar results were reported for the reaction of ketones or aldehydes with a $Ga(OTf)_3/R_3SiH$ system.[57] Since electrophilic silicon atoms are oxophilic, this is a first indication that (stabilized) silylium ions may be present in the solution, as such species should preferably react with a C=O bond rather than with a C=C bond.

In some hydrosilylation reaction mixtures, the ^{71}Ga signal is shifted downfield from −756 ppm (**1** in *o*DFB). This probably results from interactions of the olefin or the silane with Ga^+. Such interactions can possibly explain the observation that with $HSiMe_2Et$ and 1,1-diphenylethylene, the initiation of the reaction is delayed for 8 hours, most probably due to the coordination of the phenyl moieties to Ga^+.[7,26] Yet, once started, it proceeds within half an hour to full conversion at rt (entry 10; Section 2.1.7 in ESI‡).

The reaction with diolefins like 1,5-hexadiene (entry 7) or 1,5-COD resulted in the formation of a crude mixture of products, suggesting the presence of highly reactive intermediates.

Adding electron richer arenes to $[Ga(PhF)_2][pf]$. Employing very weakly basic and nucleophilic, but polar *o*DFB with a dielectric constant of $\varepsilon_r = 13.38$ [66] as a solvent is crucial for the

reaction. The addition of more coordinating solvents slowed down the reaction. For example, when the hydrosilylation of 1-hexene with $HSiMe_3$ (10 mol% of **1**) was repeated in *o*DFB with 10 vol% of slightly electron-richer PhF (= *ca.* 90 equivalents PhF referred to **1**), it took more than 20 h until 90% of the olefin was hydrosilylated. The reaction was further slowed down to 40% conversion after 11 days at rt, when only 10 vol% toluene (= *ca.* 80 equivalents toluene referred to **1**) was added to the reaction mixture.

As typical donor–acceptor complexes, the stability of $[Ga(arene)_x]^+$ complexes increases with the increase in π-basicity of the arene ligands. Consequently, in a mixture of aromatic solvents, the $[Ga(arene)_x]^+$ complex with the more π-basic ligand is always observed in solutions by NMR spectroscopy, as also supported by quantum chemical calculations.[7,15] Evidently, the Ga^+ ions have to be nearly "naked" in solution to initiate the hydrosilylation of olefins.

Mechanistic DFT investigation: Ga^+-centered reaction?

The formation of *anti*-Markovnikov addition products is also typically observed with transition metal catalysts. This is rationalized by the widely accepted and thoroughly investigated Chalk–Harrod mechanism,[67] involving oxidative addition of a transition metal into the H–Si bond, hydrometalation and reductive elimination. Thus, we first assumed that the Ga^+-catalyzed hydrosilylation proceeds *via* a similar mechanism. This is plausible in light of the $4s^24p^0$ electron configuration of Ga^I, principally allowing for transition metal or silylene[33]-like reactivity. In line with this, oxidative addition of neutral or anionic Ga^I species into covalent bonds has been reported for a multitude of different covalent bonds.[31] However, to the best of our knowledge, oxidative addition of cationic, unsupported Ga^I arene complexes into element–element bonds has not been proven experimentally so far. In order to add oxidatively into a covalent bond, a narrow HOMO/LUMO gap and energetically high lying occupied frontier orbitals are required. Therefore, the use of anionic ligands, *e.g.* in $Ga^I[^{Dipp}NacNac]$, typically facilitates oxidative addition of the resulting neutral Ga^I compounds in confined environments.[27,29,31]

A Ga^+-centered Chalk–Harrod mechanism. We analyzed the oxidative addition of $[Ga(oDFB)]^+$ into the H–Si bond of $HSiMe_3$ computationally to evaluate as to whether a Chalk–Harrod-like mechanism can be invoked by almost "naked" Ga^+.§ The mechanism and activation barriers were calculated with propylene as a model substrate at the RI-BP86(D3BJ)/def2-TZVPP level of theory. The resulting energy profile for a Chalk–Harrod-like reaction with Ga^+ as the catalyst is shown in Scheme 1. The accuracy of the method was confirmed by benchmark-coupled cluster calculations (*vide infra*). All calculated activation barriers are listed in the ESI.‡

With activation barriers surpassing 200 kJ mol^{-1}, the computational study strongly suggests that the oxidative addition of *o*DFB-complexed Ga^+ into the H–Si bond is not possible under ambient conditions. As expected, the reductive elimination of the cationic gallium species is slightly less disfavored, but activation barriers are still prohibitive, especially since single-point calculations with the gold standard CCSD(T) at the basis set limit and our model chemistry RI-BP86(D3BJ)/def2-TZVPP do not differ by more than 14 kJ mol^{-1} and also the effect of solvating the system with the COSMO model only changes the energetics by less than 10 kJ mol^{-1} (Section 6.2.1 in ESI‡).

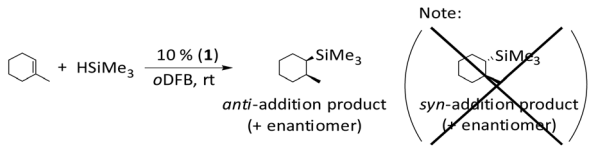

Scheme 2 The *anti*-addition product of $HSiMe_3$ and 1-methylcyclohexene is formed exclusively instead of the *syn* product. Since the starting materials are achiral, the chiral reaction product is racemic.

Further experimental investigations on the mechanism

Substrate with two enantiotopic half-spaces. To gain more insights into the reaction mechanism, we set out to determine the stereochemistry of the silane addition. To this end, we chose a substrate with two enantiotopic half-spaces, *i.e.* 1-methylcyclohexene (entry 5 in Table 1). As expected, the *anti*-Markovnikov product was formed. More importantly, the $^1H,^1H$-NOESY NMR study of the $HSiMe_3$/1-methylcyclohexene/**1** reaction mixture revealed that the H and $SiMe_3$ moieties add *anti* across the olefinic double bond (Scheme 2).

This implies that the H and $SiMe_3$ moieties add in a stepwise reaction sequence, which effectively rules out the Chalk–Harrod mechanism and underscores the theoretical calculations.

Reactions between 1 and silane: low-temperature NMR-study. With 0.1 equivalents of **1**, pronounced gas evolution was observed during hydrosilylation reactions, as well as the formation of a metallic precipitate. We thus assumed that a redox reaction between the silane and **1** could take place.

This prompted us to examine a mixture of **1** and $HSiMe_3$ in *o*DFB in some detail by NMR spectroscopy. The components were mixed at −40 °C in a 1.0 : 4.8 ratio, and the NMR spectrum

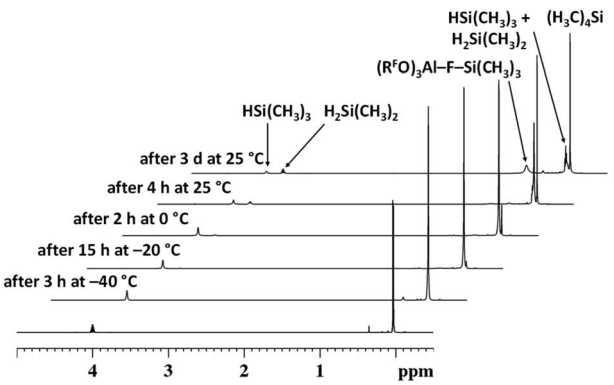

Fig. 2 From bottom to top: ^1H NMR-spectra of $HSiMe_3$ in *o*DFB at 298 K (300.18 MHz), $HSiMe_3$/**1** (4.8 : 1.0) after 3 h at 233 K, after 15 h at 253 K, after 2 h at 273 K, after 4 h at 298 K and after 3 d at 298 K (all 400.17 MHz). Signal intensities were normalized to the *o*DFB signal at 6.96 ppm (not shown). The signal at 0.35 ppm is caused by traces of $Cl–SiMe_3$ in the $HSiMe_3$ solution.

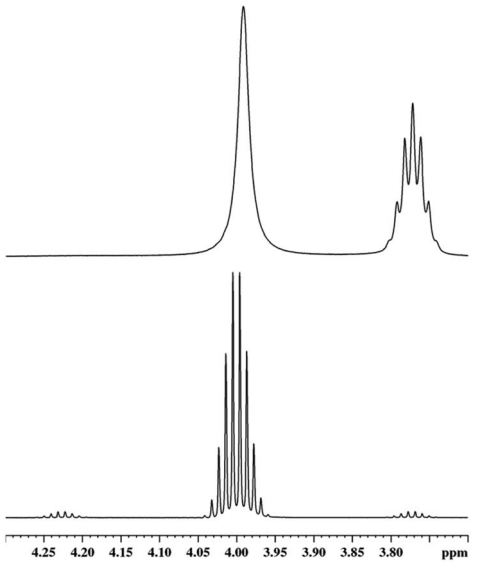

Fig. 3 ^{1}H NMR signal (400.17 MHz, *o*DFB, 298 K) of the H–Si hydrogen atom in $HSiMe_3$ (bottom) and in a $HSiMe_3$/**1** (4.8 : 1.0) mixture (top) in *o*DFB. On the top right, one notes the H–Si septet-signal of H_2SiMe_2; see text.

at this temperature showed no direct sign of reaction between the components. Yet, the coupling constant $^{3}J_{SiH,CH}$ could not be resolved (*vide infra*). Slowly increasing the temperature allowed for reaction monitoring. ^{1}H NMR spectra recorded at different temperatures are displayed in Fig. 2.

Above and at 0 °C, the formation of H_2SiMe_2 and $SiMe_4$ is observed. These species must be formed due to a ligand exchange of H and Me groups. ^{19}F NMR spectra show that, at room temperature, the $[pf]^-$ anion is quantitatively converted into perfluorinated epoxide $F_2C(O)C(CF_3)_2$ and $Me_3Si–F–Al(OR^F)_3$ (Section 2.3.1 in ESI‡). These compounds are the typical decomposition products of the $[pf]^-$ anion in the presence of a $[SiMe_3]^+$ silylium ion.[68,69] Additionally, the presence of silylium ions would easily account for the observed ligand redistribution.[70–73] Note that the underlying mechanism has been investigated in detail.[74,75] Consequently, the fact that aryl ligands display a greater migration tendency[75] probably explains why the attempted hydrosilylation with H_3SiPh or H_2SiPh_2 and **1** led to extensive ligand redistribution. In line with this, we isolated crystals of $SiPh_4$ in a mixture of H_2SiPh_2 and **1**.

Another evidence for the presence of silylium cations is the fact that the $^{3}J_{H,H}$ coupling constant in $HSiMe_3$ in a mixture of $HSiMe_3$ and **1** in *o*DFB is obviously reduced (Fig. 3). This is a general feature and also holds for a $HSiEt_3$/**1** mixture in *o*DFB (Section 2.3.2 in ESI‡).

The signal of the Si–**H** hydrogen atom in $HSiMe_3$ is not only broadened, indicating chemical exchange, but its full width at half maximum of 8.0 Hz does not allow to cover fully the original multiplet, which is at least 11.5 Hz broad at the same height. Hence, the absolute value of the $^{3}J_{H,H}$ coupling constant must be reduced, which can only occur when the hydrogen atoms are exchanged between different silicon atoms. Although the splitting pattern in the resonance of the Si–H group of H_2SiMe_2 is still resolved, there is chemical exchange between H_2SiMe_2 and $HSiMe_3$, which is demonstrated in ^{1}H EXSY NMR spectra (Section 2.3.1 in ESI‡). In the same spectrum, in the area of the $\mathbf{H}_3C–Si$ groups, additional exchange processes between Me_3SiH and other species containing Me_3Si groups, mainly $Me_3Si–F–Al(OR^F)_3$, can be observed.

In addition, the ^{71}Ga NMR signal disappears in $HSiR_3$/**1** (R = Me, Et) mixtures and a metallic mirror forms inside the NMR tube (Section 5 in ESI‡), indicating that the Ga^+ ions were reduced to elemental gallium. In agreement with this, a new ^{1}H NMR signal at 4.5 ppm could be ascribed to H_2, in line with the results from gas chromatography (*vide infra*).[76] In a mixture of **1** and $HSiEt_3$, the analogous reactions were observed by NMR spectroscopy (Section 2.3.2 in ESI‡). Moreover, crystals of $Et_3Si–F–Al(OR^F)_3$ were isolated from a concentrated solution of **1** and $HSiEt_3$ in *o*DFB. A balanced reaction equation and molecular structure of $Et_3Si–F–Al(OR^F)_3$ are shown in Scheme 3. The structural parameters are comparable to those found in $Me_3Si–F–Al(OR^F)_3$ [68] and $^{t}Bu_3Si–F–Al(OR^F)_3$,[77] identifying an "ion-like" silylium complex.[78]

Investigations towards the formation of elemental gallium. To gain a deeper understanding of the reaction between the silane and **1**, we identified the gaseous and solid side products by gas chromatography and scanning transmission electron microscopy (STEM), respectively. As apparently **1** and a hydrosilane undergo a redox reaction, we aimed to analyze and verify the oxidizing potential of Ga^+ by electrochemical methods. The results are included in Fig. 4.

The gas formed upon mixing **1** and a silane was unambiguously identified as H_2 by gas chromatography (Fig. 4a). Adding $HSiMe_3$ or $HSiEt_3$ to a solution of **1** in *o*DFB resulted in the almost immediate formation of H_2, whereas addition of $HSiEt_3$ to a mixture of **1** and 1-hexene in *o*DFB resulted in a slightly slower gas evolution (Section 3.1 in ESI‡). This is probably due

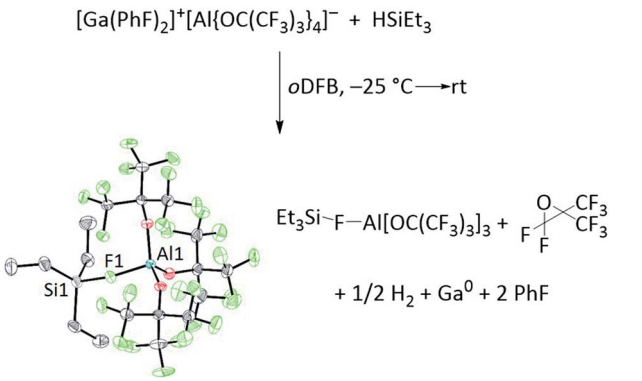

Scheme 3 Formation and molecular structure of $Et_3Si–F–Al[OC(CF_3)_3]_3$ in a mixture of **1** and $HSiEt_3$. All atoms were drawn with anisotropic thermal ellipsoids at the 50% probability level. Hydrogen atoms and a minor disorder in the $Al(OR^F)_3$-part were omitted for clarity. Selected bond lengths [pm] and angles [°] of the ordered sections of the molecule: F1–Si1: 173.18(17), F1–Al1: 178.82(16), Al1–O: 169.2(5)–170.80(19), Si1–F1–Al1: 157.67(9). Sum of C–Si–C angles: 346.44(14)°.

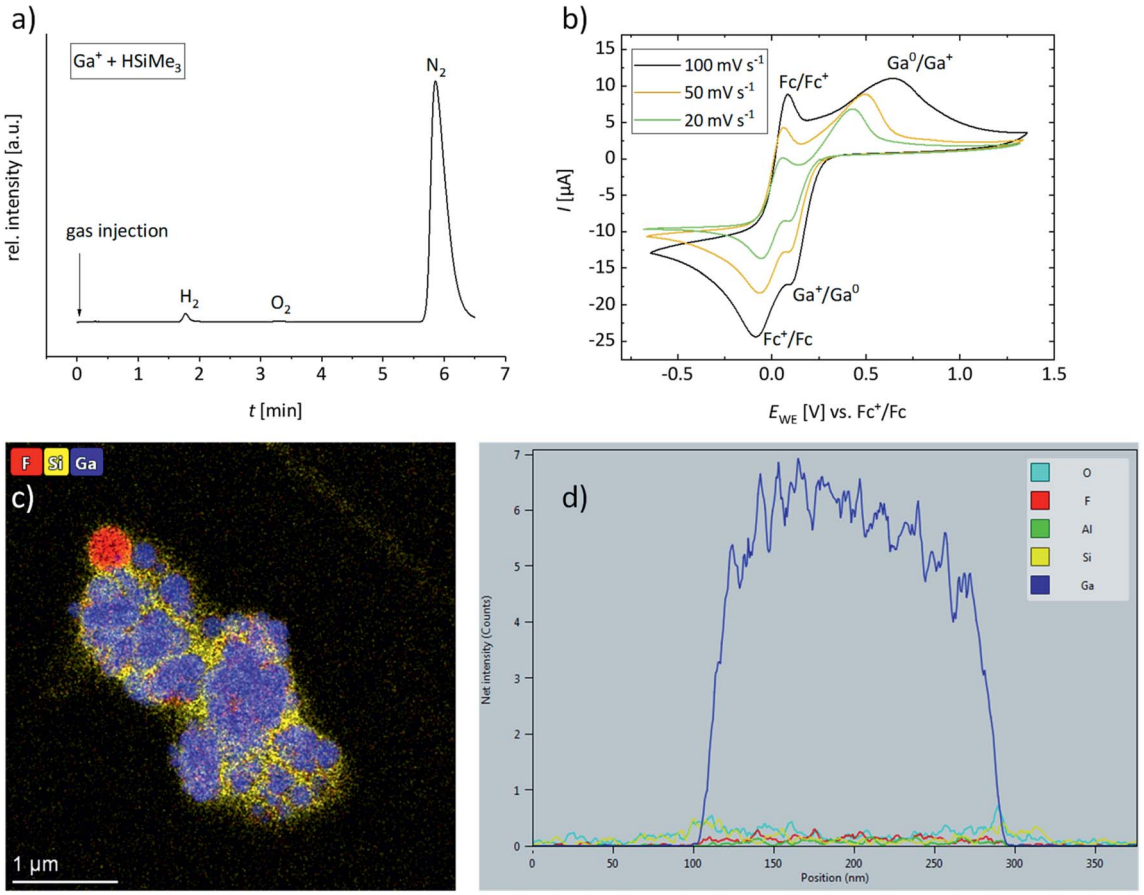

Fig. 4 Gas chromatogram of the gas space above the reaction solution of $HSiMe_3$ and **1** (5.8 : 1.0) in *o*DFB (a). Cyclic voltammograms of **1** and [Fc][*pf*] in *o*DFB (0.005 M, respectively) at rt and at a Pt working electrode (WE); measured with different scan rates. [NBu_4][*pf*] (0.1 M) was used as a conducting salt (b). STEM element maps (fluorine, silicon and gallium) associated with the dark-field image of the residue of the $HSiMe_2Et$/1-hexene/**1** (2.2 : 1.0 : 0.1) reaction mixture (c) and background-corrected EDX line scan for the elements O, F, Al, Si, and Ga in the same sample across a Ga-rich particle (d). The F-rich area in (c) (top left) probably results from traces of non-vaporized *o*DFB.

to coordination of olefin molecules to Ga^+, which have to be displaced by the silane. No H_2 could be detected in solutions of **1** and an olefin in *o*DFB.

The cyclic voltammograms of a 0.005 M solution of **1** in *o*DFB (Fig. 4b) reveal that the redox potential of Ga^+/Ga^0 is more positive than the potential of $[Fc]^+/[Fc]$ in *o*DFB (Fc = ferrocene). The exact redox potential $E_{1/2}$ is difficult to determine, since it depends on the scan rate (*e.g.* $E_{1/2}$ = +0.26 V *vs.* Fc^+/Fc for 20 mV s^{-1}, and $E_{1/2} \approx$ +0.37 V *vs.* Fc^+/Fc for 100 mV s^{-1}). Thus, the conversion of Ga^+ into Ga^0 is electrochemically not fully reversible. For further experimental proof of this high and positive Ga^+/Ga^0 potential, **1** was added to the orange-yellow solution of ferrocene and the mixture turned blue immediately, indicating oxidation of neutral ferrocene to ferrocenium (Section 5 in ESI‡). Thus, we showed that Ga^+, typically viewed as a subvalent reductant,[79] can act as an oxidizing agent with a formal potential even higher than that of Fc^+. Note that ferrocenium salts are typically used as chemical oxidants.[80] Interestingly, no electrochemical oxidation of Ga^+ to Ga^{3+} was observed (Section 3.2 in ESI‡).

Unfortunately, no cyclic voltammograms of $HSiEt_3$ could be recorded under the same conditions. Yet, it has already been shown in 1958 that $HSiEt_3$ can reduce inorganic halides with the formation of H_2, elemental metal and $XSiEt_3$ (X = Br and Cl).[81] Silanes and related H–Si containing compounds have been employed as reducing agents for more oxidizing metal ions, *e.g.* for Rh^{3+},[82] Pd^{2+},[82,83] Pt^{4+},[82,83] Cu^{2+},[84] Au^{3+},[82,83] $[AuCl_4]^-$,[85] and Ag^+[83,86] ions, in order to obtain the respective metal nanoparticles. Besides this, hydrosilanes act as reducing agents in redox-initiated cationic polymerization reactions.[87] It is known that Ga^{III} can oxidize organic compounds under H_2 formation, however, without being reduced to elemental gallium.[88] Yet, the use of naked "Ga^+" as an oxidizing agent towards silanes is new. Moreover, in *o*DFB, $HSiMe_3$ reacts with the oxidizing salts NO[*pf*] and Ag[*pf*] in a similar manner to **1**, *i.e.* under H_2 formation, ligand scrambling and $[pf]^-$ anion decomposition (Sections 2.3.3 and 2.3.4 in ESI‡). This supports the notion that Ga^+, too, acts as an oxidizing agent towards silanes. The metallic precipitate formed during a hydrosilylation reaction was isolated in small amounts and was analyzed by STEM-analysis. It includes largely metallic gallium particles (Ga^0 by STEM-analysis, Fig. 4c and d) embedded in a Ga-poor but O- and Si-rich matrix, confirming that a redox reaction between **1** and hydrosilanes takes place.

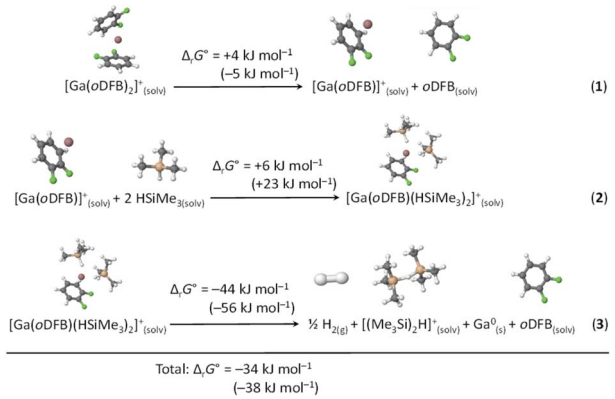

Scheme 4 Calculated Gibbs free energies $\Delta_rG°$ (*o*DFB solution, calculated with the COSMO model, $\varepsilon_r = 13.38$ [66]) for the dissociation of $[Ga(oDFB)_2]^+$ (reaction (1)), subsequent addition of two $HSiMe_3$ molecules to yield $[Ga(oDFB)(HSiMe_3)_2]^+$ (reaction (2)), and its decomposition to give H_2, Ga^0, *o*DFB and $[(Me_3Si)_2H]^+$ (reaction (3)). The Gibbs free energies were calculated at the RI-BP86(D3BJ)/def2-TZVPP level at 298 K (values in parentheses: RI-B3LYP(D3BJ)/def2-TZVPP). The optimized structures of the involved species are included.

As already pointed out, the addition of toluene slows down the hydrosilylation reaction initiated by **1** in *o*DFB. Toluene is more electron-rich and the arene molecules may coordinatively saturate the Ga^+ ions, thereby preventing the coordination of silane molecules and thus the suspected redox reaction between silane and univalent gallium. Moreover, the hydrosilylation with HSi^iPr_3 and initiated by **1** is extremely slow even in *o*DFB (entry 18 in Table 1). This is a hint that the reaction between silane and Ga^+ is dependent on a coordinatively unsaturated Ga^+ cation, and that the steric demand of ligands may also play a major role in the reaction kinetics. Possibly, in order to initiate the redox reaction, at least two silane molecules have to coordinate to Ga^+. Therefore, it seems plausible that an inner sphere mechanism is operative and that the steric bulk of the ^{i}Pr groups disfavors the redox reaction.

Computational analysis of the redox reaction between 1 and silane, catalytic cycle

The thermodynamics of the postulated redox reaction between Ga^+ and $HSiMe_3$ were examined by DFT methods. It was assumed that $[Ga(oDFB)(HSiMe_3)_2]^+$ and, subsequently, $[(Me_3Si)_2H]^+$ are formed. Optimized structures and their underlying thermodynamics are shown in Scheme 4. The species $[(Me_3Si)_2H]^+$ was chosen as a silylium equivalent, since silylium ions $[R_3Si]^+$ are highly reactive electrophiles[89,90] and already form Lewis acid–base adducts with moderate to weak nucleophiles like toluene.[11,12,91] Such silylium-silane adducts, or bissilylhydronium ions, are well known[92–94] and due to the great excess of silane and the non-resolved $^3J_{H,H}$ coupling in mixtures of **1** and a hydrosilane, it is plausible to assume that such species are present in an *o*DFB solution. Computational analysis suggests that the bissilylhydronium ion $[Me_3Si–H–SiMe_3]^+$ is more stable than $[Me_3Si(oDFB)]^+$ adducts by *ca.* 50 kJ mol^{-1} (Section 6.2.3 in ESI‡), which is in agreement with previous experimental findings.[90,93,94]

It follows from the computational analysis that the postulated reaction is thermodynamically possible, with the formation of gaseous H_2 and elemental gallium clearly being the driving force. In addition, the *o*DFB/silane ligand exchange is expected to be a fast process in the solution. Moreover, only a smaller fraction of the silane molecules would have to react according to the reaction in Scheme 4, since we propose that the supported silylium ions are the genuine, catalytically very active, species.

Ga^+ initiation and proposed catalytic hydrosilylation cycle. The presented results indicate that supported silylium ions are present in mixtures of **1** and silanes $HSiR'R_2$ (R, R′ = H, alkyl, and aryl) in *o*DFB. Apparently, these silylium ions are the actual catalysts in the herein investigated Ga^+-induced hydrosilylation of olefins. Accordingly, it is well known that silylium ions add across olefinic double bonds and that silanes can act as hydride donors for the resulting β-silyl carbocations.[95–97] Thus, the univalent gallium ions serve as initiators rather than catalysts. Interestingly, in reaction mixtures with olefins, the $[pf]^-$ anion is only partly decomposed to $R_3Si–F–Al(OR^F)_3$. In fact, anion decomposition is barely observed when carrying out the reactions at rt and employing less than 10% of **1**. This is probably due to the great surplus of olefin, which coordinates to Ga^+ and slows down the redox reaction with the silane. By contrast, complete anion decomposition is observed when no olefin is present in solution (*cf.* ^{19}F NMR spectra in Section 2.3 in ESI‡). A complete catalytic cycle for the Ga^+-initiated hydrosilylation of olefinic double bonds is proposed in Scheme 5.

Since silylium ions are highly reactive species that usually cannot be observed in the solution,[98] we attempted to observe β-silyl carbocations instead (**9** in Scheme 5). We chose 1,1-diphenylethylene as a suitable substrate, due to the high stability of the intermediate β-silyl carbocation.[95] Unfortunately, no intermediates were observed in a mixture of **1**, $HSiEt_3$ and 1,1-diphenylethylene (Section 2.1.9 in ESI‡), even below 0 °C. The accumulation of β-silyl carbocations is probably prevented

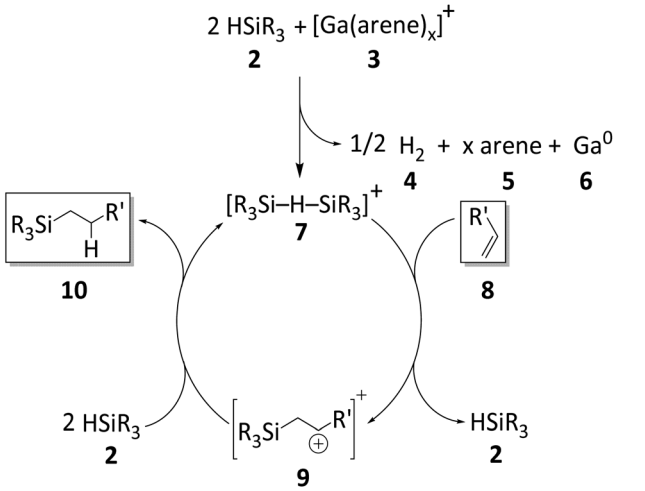

Scheme 5 Proposed catalytic cycle for the hydrosilylation of olefins initiated by Ga^+ (arene = *o*DFB or PhF). The olefin **8** and the hydrosilylation product **10** are highlighted.

Table 2 Initiator concentration, reaction time and conversion for the $[Ph_3C][pf]$-initiated hydrosilylation of 1-hexene (c = 0.11 M) with $HSiMe_3$

#	Molar ratio silane : olefin : $[Ph_3C][pf]$	Reaction time	Yield[a]
1	1.1 : 1.0 : 0.01	<5 min	>97%
2	1.1 : 1.0 : 0.005	<5 min	>97%
3	1.1 : 1.0 : 0.003	8 min	>97%
4	2.0 : 1.0 : 0.002	1 h	>97%[b]
5	1.0 : 1.0 : 0.002	1 h	93%[b]

[a] Determined by ^{1}H NMR spectroscopy, referred to the deficit substrate. [b] The rate of the reaction with 0.2 mol% $[Ph_3C][pf]$ varies significantly and is somewhat erratic: full conversion was observed after 1 h to 5 d.

by the fact that silylium ions are generated *in situ* together with excess silane that acts as an available hydride donor and reduces the lifetime of the carbocation.

The exact mechanism of the initial redox reaction is not entirely clear. For example, a direct one-electron reduction of Ga^+ is conceivable as well as a Piers–Oestreich-like reaction. The Piers–Oestreich mechanism has been extensively studied and applies to hydrosilylation reactions of various substrates with neutral or cationic Lewis acids.[36,49–51,55,56,60,99] If the Piers–Oestreich mechanism is applied to the herein investigated reaction, Ga^+ and a silane molecule would form adducts of the type $[Ga–H–SiR_3]^+$, which are subsequently attacked by the olefin, forming β-silyl carbocations and "GaH". The latter would decompose into elemental gallium and H_2, while the β-silyl carbocations would initiate the reactions of the catalytic cycle shown in Scheme 5. Thus, a Piers–Oestreich-like mechanism and a direct initial redox reaction would essentially lead to the same outcome and both mechanisms account for the observations and experimental results presented herein. However, quantum chemical calculations suggest that, even when the formation of a Si–C bond in the β-silyl carbocation is considered, the formation of an intermediate gallium hydride is endergonic by *ca.* 150 kJ mol^{-1} in *o*DFB (Section 6.2.4 in ESI‡). This is ultimately due to the weakness of the Ga–H bond especially in weakly coordinating environments[19,66] and due to the relative stability of Ga^+ cations compared to silylium ions or carbocations. Besides this, the fact that Ga^+ oxidizes ferrocene suggests that Ga^+ acts as a one-electron oxidizing agent. Thus, even though it cannot be ruled out experimentally, it seems rather unlikely that a classical Piers–Oestreich mechanism is operative in the system **1**/$HSiR_3$/olefin.

Verification of silylium ion catalysis by initiation with trityl aluminate

The validity of the mechanism shown in Scheme 5 is further supported by the fact that catalytic amounts of $[Ph_3C][pf]$[100] instead of **1** also initiate hydrosilylation reactions at room temperature. The reaction between trityl salts and hydrosilanes is known as the Bartlett–Condon–Schneider reaction and is widely employed in order to generate silylium ions.[70,73,75,95,96,101] As shown in Table 2, with 1.0 mol%, 0.5 mol% and 0.3 mol% of

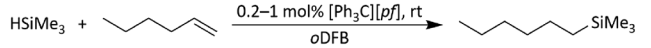

Scheme 6 Hydrosilylation of 1-hexene with $HSiMe_3$, initiated by $[Ph_3C][pf]$ and catalyzed by silylium ions.

$[Ph_3C][pf]$, the reaction between 1-hexene and $HSiMe_3$ (Scheme 6) is almost immediately completed and also yields the *anti*-Markovnikov product (*cf.* entries 1–3 in Table 1). Using 0.2 mol% is less reliable. When employing such low concentrations of $[Ph_3C][pf]$, the reactivity of this system is probably influenced by trace impurities, due to the high reactivity of both the trityl cation[102] and silylium ions.[71,89,90]

The fact that the hydrosilylation reaction is considerably faster with $[Ph_3C][pf]$ than with **1** is not surprising and indicates that $[Ph_3C]^+$ is more efficient in generating silylium ions *in situ* than Ga^+. Partial anion decomposition to the perfluorinated epoxide $F_2C(O)C(CF_3)_2$ and to $Me_3Si–F–Al(OR^F)_3$ (Section 2.1.17 in ESI‡) again points to the presence of silylium ions, but does not affect the hydrosilylation reaction.

Hydrodefluorination with the 1/$HSiEt_3$ and the $[Ph_3C][pf]$/$HSiEt_3$-system

Silylium catalysis is a growing research field and has already become a powerful tool for various chemical transformations.[71,89,90,103] For example, the concept of mild, $[Et_3Si][WCA]$-catalyzed hydrodefluorination (WCA = $[B(C_6F_5)_4]^-$ or carborate), *i.e.* the transformation of a C–F bond into a C–H bond was introduced by Ozerov.[98,104] Such transformations are challenging, due to the strength of C–F bonds.[105] In the systems presented by Ozerov, silylium ions abstract C(sp^3)-bound fluorine atoms and stoichiometric amounts of hydrosilanes serve as hydride donors for the resulting carbocations, thus regenerating the catalytically active silylium ions.

In order to further probe whether silylium ions are present in the mixture of **1** and a hydrosilane in *o*DFB, we tested whether hydrodefluorination reactions of C(sp^3)–F bonds at room temperature are possible with this system. Considering the results presented in the previous sections, it is no surprise that the $HSiEt_3$/**1** mixture indeed induces hydrodefluorination. This was exemplarily demonstrated with four different, representative substrates, *i.e.* 1-fluorobutane, trifluorotoluene, 1-fluoroadamantane and *n*-perfluorohexane (Section 2.2 in ESI‡). With trifluorotoluene, a mixture of diphenylmethane derivatives was formed, whereas with 1-fluorobutane, the formation of butane and of an *s*-butylated *o*DFB derivate was observed (entries 1 and 2 in Table 3). The hydrodefluorination of 1-fluoroadamantane proceeded smoothly and quantitatively yielded adamantane (entries 3 and 4). We employed 1-fluoroadamantane since it serves as a benchmark substrate for hydrodefluorination reactions, in order to compare catalytic efficiencies of Lewis-acidic systems.[106–118]

The attempted hydrodefluorination of *n*-perfluorohexane with **1**/$HSiEt_3$ was unsuccessful (entry 5). The inertness of perfluorinated alkanes in silylium-catalyzed hydrodefluorination reactions is well documented[98,119] and can probably be

Table 3 Hydrodefluorination reactions carried out in *o*DFB with [Ga(PhF)$_2$][*pf*] (**1**) and HSiEt$_3$. The C–F conversion as determined by NMR spectroscopy is given

#	R–F	Molar ratio HSiEt$_3$: R–F : **1**	*c* (R–F) [M]	Reaction time (temperature)	Main products	C–F conversion[a]
1	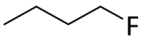	1.1 : 1.0 : 0.04	0.62	10 h (5 °C)	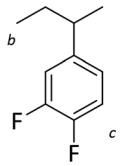	>97%
2	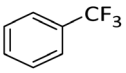	4.0 : 1.0 : 0.05	0.48	17 h (rt)	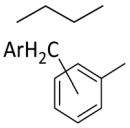	96% (product mixture)
3		2.8 : 1.0 : 0.05	0.18	<3 min (rt)		>97%
4		2.0 : 1.0 : 0.001	0.26	14 h (rt)		95%
5	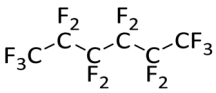	15 : 1.0 : 0.56	0.21	14 d (rt)	No reaction[d]	—

[a] Determined by ^{19}F NMR spectroscopy (C–F conversion = *c* (Et$_3$Si–F)/*c* (R$_3$C–F + Et$_3$Si–F)). [b] Additionally, traces of the regioisomer with the ^{s}Bu group in 2 position of the aromatic ring were detected. [c] The *s*-butylated *o*DFB derivate and ^{n}butane are formed in a 0.3 : 1.0 ratio. [d] Anion decomposition was observed.

attributed to the strong –I effect of the adjacent fluorine atoms, which would destabilize intermediate alkylcarbocations.

The reaction products indicate that with 1-fluorobutane, trifluorotoluene and 1-fluoroadamantane, the intended hydrodefluorination reactions took place. Yet, the hydrodefluorination of trifluorotoluene was accompanied by Friedel–Crafts reactions and, for 1-fluorobutane, additionally by Wagner–Meerwein rearrangements. It is revealing that, in the reaction with 1-fluorobutane, the aromatic solvent is *s*-butylated instead of *n*-butylated (entry 1), since primary carbocationic species are usually less stable than secondary ones. Therefore, Friedel–Crafts reactions with alkylating agents often lead to unexpected products with rearranged alkyl substituents.[120]

The hydrodefluorination of trifluorotoluene yielded a mixture of diphenylmethane derivatives instead of the expected product, toluene (entry 2). However, toluene is most likely formed initially, but, as a reasonably electron-rich aromatic compound, reacts with the intermediate carbocations in Friedel–Crafts reactions under C–C bond formation. The reaction outcome is reminiscent of the results for [Et$_3$Si][carborate]-catalyzed hydrodefluorination reactions with trifluorotoluene.[104,119] Interestingly, as the reaction proceeds, only CH$_3$–, CH$_2$– and CF$_3$ groups are present in the solution. No intermediates like Ar–CF$_2$H or Ar–CFH$_2$ were observed, even when only a 1.5-fold excess of triethylsilane was employed. Consequently, the abstraction of the first F-atom in trifluorotoluene is more energy-intensive than the abstraction of the next two F-atoms, in line with the decreasing C–F bond enthalpy of R–CF$_x$H$_{3-x}$ for decreasing *x*.[121] This is an important finding, since similar results were reported for the [Et$_3$Si][B(C$_6$F$_5$)$_4$]-catalyzed hydrodefluorination of PhCF$_3$ by Ozerov.[98] In a side reaction, the hydride source, HSiEt$_3$, probably reacts with the protons released in the Friedel–Crafts reactions. This results in the formation of "[SiEt$_3$]$^+$", and of H$_2$, which is underpinned by an intense ^{1}H NMR signal of H$_2$ at *ca.* 4.50 ppm.

Gratifyingly, 1-fluoroadamantane was hydrodefluorinated in an almost immediate reaction at rt, yielding adamantane quantitatively (entry 3). It is noteworthy that the hydrodefluorination reaction with our herein presented system HSiEt$_3$/**1** is remarkably faster than the reaction with highly Lewis-acidic, but neutral, bis(catecholato)silanes recently presented by Greb,[114] again indicating the presence of highly reactive species in the reaction solution. It is difficult to estimate turnover numbers (TON) or turnover frequencies (TOF) for our catalytic system, since the exact concentration of the silylium ions, the supposed catalysts, is not known. Even when assuming that every Ga$^+$ (c = 8.4 mM) converts one silane molecule in a silylium ion, the TOF is greater than 0.1 s^{-1} at room temperature. This value is significantly higher than the

TOF for the bis(catecholato)silanes in the analogous reaction (c = 7.5 mM; *ca.* 2.5 × 10^{-3} s^{-1} at 75 °C for the most active catalyst after 3 h). Typically, for catalytically active Lewis acid/hydride donor systems, TOF values between 1 × 10^{-4} s^{-1} and 7 × 10^{-2} s^{-1} for the hydrodefluorination of 1-fluoroadamantane are reported, underlining the high efficiency of the **1**/$HSiEt_3$ system in hydrodefluorination reactions.[106–118] However, the hydrodefluorination of this substrate is considerably faster than any other Ga^{I}-initiated hydrosilylation or hydrodefluorination reaction presented herein. Thus, the reaction may follow a different mechanism with this particular substrate. Remarkably, the reaction is also catalyzed by 0.1 mol% of **1** (c = 0.29 mM; entry 4) at rt.

In this context, it has to be noted that the initiation reaction of the hydrodefluorination reaction sequence could similarly involve a fluoride abstraction by Ga^{+}, resulting in the formation of "GaF" and a carbocation, which would subsequently react with a silane molecule to yield the hydrodefluorination product and a silylium ion. Either way, the results of the hydrodefluorination reactions with **1**/$HSiEt_3$ again imply that reactive cations, *i.e.* carbenium and silylium ions, are the reaction intermediates in Ga^{+}-initiated hydrosilylation and hydrodefluorination reactions. In order to further support this thesis, we conducted another hydrodefluorination experiment with 1-fluoroadamantane, $HSiEt_3$ and $[Ph_3C][pf]$ (c = 0.53 mM) in a 1.0 : 2.0 : 0.002 ratio. Complete hydrodefluorination was observed within 15 minutes, which corresponds to an exceptionally high TOF of at least 0.5 s^{-1}.

These are important findings as it was often assumed that the use of carborate or borate anions is mandatory for silylium ion catalysis, since other anions are less robust towards these strong electrophiles.[89,90] In line with this, to the best of our knowledge, the only alternative Ga^{I} species that initiate hydrosilylation reactions are a carborate and a borate salt.[19] Gratifyingly, our results indicate that silylium catalysis is also possible with the straightforward and very large-scale accessible $[pf]^{-}$ anion (>100 g in one batch).[20,122] For example, the Ga^{I} salt **1**[15] and the trityl salt $[Ph_3C][pf]$[100] can easily be synthesized and the latter, obviously a very potent initiator for silylium-catalysis, is even commercially available.[123]

Conclusion

We demonstrated that the system $[Ga(PhF)_2][pf]$/$HSiR_3$ (R = alkyl) initiates hydrosilylation reactions of olefinic double bonds in *o*DFB under mild conditions. Pronounced ligand scrambling is observed with phenylsilanes and, if excess silane is applied, with the less symmetrical silane $HSiMe_2Et$, which makes the hydrosilylation less selective with these silanes. A very slow reaction was observed with $HSi^{i}Pr_3$. Additionally, efficient hydrodefluorination of $C(sp^3)$–F bonds works with $[Ga(PhF)_2][pf]$/$HSiEt_3$ in *o*DFB. We proposed that the reaction sequence, for both hydrosilylation and hydrodefluorination, is initiated by a redox reaction between Ga^{+} and the silane, releasing Ga^{0}, H_2 and a $HSiR_3$-masked silylium ion. The masked or supported silylium ions probably act as the actual catalytically active species and Ga^{+} as the initiator. To the best of our knowledge, this is the first systematic report of the use of subvalent gallium as an oxidizing agent, which adds a new exciting facet to the chemistry of Ga^{+}. The surprisingly high oxidative potential of Ga^{+} in *o*DFB was confirmed by cyclic voltammetry, and we showed that Ga^{+} oxidizes ferrocene in *o*DFB. In addition, our results suggest that (masked) silylium ion catalysis is possible with the $[pf]^{-}$ anion. Consequently, highly efficient hydrosilylation of 1-hexene and hydrodefluorination of 1-fluoroadamantane were observed using only 0.2 mol% $[Ph_3C][pf]$. We anticipate that the use of the $[pf]^{-}$ anion could simplify silylium catalysis in the future and promote the development of new silylium-catalyzed reactions. Sparked by this and other unusual chemistry, the application and understanding of $[Ga(PhF)_2][pf]$ in catalytic transformations is currently one of the main research interests in our laboratory.

Data availability

Electronic supplementary information (ESI) is available. Full experimental details, 1D- and 2D NMR spectra of the reactions are deposited. Details to the quantum chemical calculations are given together with the results of gas chromatographic, cyclic voltammetry, STEM/EDX measurements and crystallographic details.

Author contributions

I. K., A. B. and K. G. conceived the experiments. A. B., K. G. and A. H. performed the experiments. H. S. measured the NMR spectra, all authors analyzed and discussed the experimental data. A. B. and I. K. co-wrote the paper and edited the manuscript.

Conflicts of interest

There are no conflicts to declare.

Acknowledgements

This work was supported by the Albert-Ludwigs-Universität Freiburg and by the DFG in the Normalverfahren. We would like to thank Harald Scherer and Fadime Bitgül for the measurement of the NMR spectra, Dr Ralf Thomann for the collection of the STEM and EDX data and Dr Daniel Kratzert and Dr Burkhard Butschke for their support regarding single X-ray crystallography. The authors acknowledge support by the state of Baden-Württemberg through bwHPC and the German Research Foundation (DFG) through grant no. INST 40/467-1 and 575-1 FUGG (JUSTUS1 and 2 cluster). The use of the STEM-EDX set up, acquired through the BMBF project EDELKAT (FKZ 03X5524), is gratefully acknowledged.

Notes and references

§ Since the reactions were carried out in *o*DFB and since the use of *o*DFB as a solvent is crucial for the reaction kinetics, $[Ga(oDFB)]^{+}$ was chosen as a model complex instead of Ga^{+} or $[Ga(PhF)]^{+}$.

1 R. J. Baker and C. Jones, *Dalton Trans.*, 2005, 1341–1348.
2 M. L. Green, P. Mountford, G. J. Smout and S. Speel, *Polyhedron*, 1990, **9**, 2763–2765.
3 G. Garton and H. M. Powell, *J. Inorg. Nucl. Chem.*, 1957, **4**, 84–89.
4 (*a*) D. Loos, E. Baum, A. Ecker, H. Schnöckel and A. J. Downs, *Angew. Chem., Int. Ed.*, 1997, **36**, 860–862; (*b*) P. Jutzi, B. Neumann, G. Reumann and H.-G. Stammler, *Organometallics*, 1998, **17**, 1305–1314; (*c*) C. Schenk, R. Köppe, H. Schnöckel and A. Schnepf, *Eur. J. Inorg. Chem.*, 2011, 3681–3685.
5 (*a*) In *Chemistry of aluminium, gallium, indium and thallium*, A. J. Downs, Blackie Acad. & Professional, London, 1st edn, 1993; (*b*) A. Schnepf and C. Doriat, *Chem. Commun.*, 1997, 2111–2112.
6 P. Dabringhaus, A. Barthélemy and I. Krossing, *Z. Anorg. Allg. Chem.*, 2021, **647**, 1660–1673.
7 H. Schmidbaur, *Angew. Chem., Int. Ed.*, 1985, **24**, 893–904.
8 B. J. Malbrecht, J. W. Dube, M. J. Willans and P. J. Ragogna, *Inorg. Chem.*, 2014, **53**, 9644–9656.
9 N. J. Hardman, B. E. Eichler and P. P. Power, *Chem. Commun.*, 2000, 1991–1992.
10 R. J. Baker, R. D. Farley, C. Jones, M. Kloth and D. M. Murphy, *J. Chem. Soc., Dalton Trans.*, 2002, 3844–3850.
11 T. A. Engesser, M. R. Lichtenthaler, M. Schleep and I. Krossing, *Chem. Soc. Rev.*, 2015, **45**, 789–899.
12 I. M. Riddlestone, A. Kraft, J. Schaefer and I. Krossing, *Angew. Chem., Int. Ed.*, 2018, **57**, 13982–14024.
13 (*a*) B. Buchin, C. Gemel, T. Cadenbach, R. Schmid and R. A. Fischer, *Angew. Chem., Int. Ed.*, 2006, **45**, 1074–1076; (*b*) B. Buchin, C. Gemel, T. Cadenbach, R. Schmid and R. A. Fischer, *Angew. Chem., Int. Ed.*, 2006, **45**, 1674.
14 J. N. Jones, C. L. Macdonald, J. D. Gorden and A. H. Cowley, *J. Organomet. Chem.*, 2003, **666**, 3–5.
15 J. M. Slattery, A. Higelin, T. Bayer and I. Krossing, *Angew. Chem., Int. Ed.*, 2010, **49**, 3228–3231.
16 R. J. Wehmschulte, *Angew. Chem., Int. Ed.*, 2010, **49**, 4708–4709.
17 S. Welsch, M. Bodensteiner, M. Dušek, M. Sierka and M. Scheer, *Chem.–Eur. J.*, 2010, **16**, 13041–13045.
18 A. Higelin, U. Sachs, S. Keller and I. Krossing, *Chem.–Eur. J.*, 2012, **18**, 10029–10034.
19 R. J. Wehmschulte, R. Peverati and D. R. Powell, *Inorg. Chem.*, 2019, **58**, 12441–12445.
20 I. Krossing, *Chem.–Eur. J.*, 2001, **7**, 490–502.
21 U. Schneider and S. Kobayashi, *Acc. Chem. Res.*, 2012, **45**, 1331–1344.
22 Z. Li, G. Thiery, M. R. Lichtenthaler, R. Guillot, I. Krossing, V. Gandon and C. Bour, *Adv. Synth. Catal.*, 2018, **360**, 544–549.
23 Z. Li, S. Yang, G. Thiery, V. Gandon and C. Bour, *J. Org. Chem.*, 2020, **85**, 12947–12959.
24 K. Glootz, A. Barthélemy and I. Krossing, *Angew. Chem., Int. Ed.*, 2021, **60**, 208–211.
25 M. R. Lichtenthaler, A. Higelin, A. Kraft, S. Hughes, A. Steffani, D. A. Plattner, J. M. Slattery and I. Krossing, *Organometallics*, 2013, **32**, 6725–6735.
26 M. R. Lichtenthaler, S. Maurer, R. J. Mangan, F. Stahl, F. Mönkemeyer, J. Hamann and I. Krossing, *Chem.–Eur. J.*, 2015, **21**, 157–165.
27 A. Seifert, D. Scheid, G. Linti and T. Zessin, *Chem.–Eur. J.*, 2009, **15**, 12114–12120.
28 C. Jones, D. P. Mills and R. P. Rose, *J. Organomet. Chem.*, 2006, **691**, 3060–3064.
29 A. Kempter, C. Gemel and R. A. Fischer, *Inorg. Chem.*, 2008, **47**, 7279–7285.
30 (*a*) R. J. Baker, C. Jones and M. Kloth, *Dalton Trans.*, 2005, 2106–2110; (*b*) R. J. Baker, C. Jones, D. P. Mills, D. M. Murphy, E. Hey-Hawkins and R. Wolf, *Dalton Trans.*, 2006, 64–72; (*c*) G. Prabusankar, A. Doddi, C. Gemel, M. Winter and R. A. Fischer, *Inorg. Chem.*, 2010, **49**, 7976–7980.
31 T. Chu and G. I. Nikonov, *Chem. Rev.*, 2018, **118**, 3608–3680.
32 C. Ganesamoorthy, D. Bläser, C. Wölper and S. Schulz, *Organometallics*, 2015, **34**, 2991–2996.
33 C. Shan, S. Yao and M. Driess, *Chem. Soc. Rev.*, 2020, **49**, 6733–6754.
34 L. D. de Almeida, H. Wang, K. Junge, X. Cui and M. Beller, *Angew. Chem., Int. Ed.*, 2021, **60**, 550–565.
35 D. Troegel and J. Stohrer, *Coord. Chem. Rev.*, 2011, **255**, 1440–1459.
36 Y. Nakajima and S. Shimada, *RSC Adv.*, 2015, **5**, 20603–20616.
37 R. J. Hofmann, M. Vlatković and F. Wiesbrock, *Polymers*, 2017, **9**, 534.
38 L. N. Lewis, J. Stein, Y. Gao, R. E. Colborn and G. Hutchins, *Platinum Met. Rev.*, 1997, **41**, 66–75.
39 L. H. Sommer, E. W. Pietrusza and F. C. Whitmore, *J. Am. Chem. Soc.*, 1947, **69**, 188.
40 (*a*) J. L. Speier, J. A. Webster and G. H. Barnes, *J. Am. Chem. Soc.*, 1957, **79**, 974–979; (*b*) R. A. Benkeser and J. Kang, *J. Organomet. Chem.*, 1980, **185**, C9–C12.
41 B. D. Karstedt, *US Pat.*, US 3775452A, 1973.
42 (*a*) B. J. Truscott, A. M. Z. Slawin and S. P. Nolan, *Dalton Trans.*, 2013, **42**, 270–276; (*b*) M. Xue, J. Li, J. Peng, Y. Bai, G. Zhang, W. Xiao and G. Lai, *Appl. Organomet. Chem.*, 2014, **28**, 120–126.
43 (*a*) J. A. Muchnij, F. B. Kwaramba and R. J. Rahaim, *Org. Lett.*, 2014, **16**, 1330–1333; (*b*) X. Xie, X. Zhang, H. Yang, X. Ji, J. Li and S. Ding, *J. Org. Chem.*, 2019, **84**, 1085–1093.
44 S. Dagorne and R. Wehmschulte, *ChemCatChem*, 2018, **10**, 2509–2520.
45 (*a*) F. Buch, J. Brettar and S. Harder, *Angew. Chem., Int. Ed.*, 2006, **45**, 2741–2745; (*b*) P. Dabringhaus, M. Schorpp, H. Scherer and I. Krossing, *Angew. Chem., Int. Ed.*, 2020, **59**, 22023–22027.
46 (*a*) P.-F. Fu, L. Brard, Y. Li and T. J. Marks, *J. Am. Chem. Soc.*, 1995, **117**, 7157–7168; (*b*) H. Schumann, M. R. Keitsch, J. Demtschuk and G. A. Molander, *J. Organomet. Chem.*, 1999, **582**, 70–82.

47 (*a*) Y. Chen, C. Sui-Seng, S. Boucher and D. Zargarian, *Organometallics*, 2005, **24**, 149–155; (*b*) A. M. Tondreau, C. C. H. Atienza, K. J. Weller, S. A. Nye, K. M. Lewis, J. G. P. Delis and P. J. Chirik, *Science*, 2012, **335**, 567–570; (*c*) Y. Liu and L. Deng, *J. Am. Chem. Soc.*, 2017, **139**, 1798–1801.

48 (*a*) K. Yamamoto and M. Takemae, *Synlett*, 1990, **1990**, 259–260; (*b*) Y.-S. Song, B. R. Yoo, G.-H. Lee and I. N. Jung, *Organometallics*, 1999, **18**, 3109–3115; (*c*) J. Chen and E. Y.-X. Chen, *Angew. Chem., Int. Ed.*, 2015, **54**, 6842–6846.

49 M. Rubin, T. Schwier and V. Gevorgyan, *J. Org. Chem.*, 2002, **67**, 1936–1940.

50 K. Jakobsson, T. Chu and G. I. Nikonov, *ACS Catal.*, 2016, **6**, 7350–7356.

51 J. M. Blackwell, E. R. Sonmor, T. Scoccitti and W. E. Piers, *Org. Lett.*, 2000, **2**, 3921–3923.

52 J. Koller and R. G. Bergman, *Organometallics*, 2012, **31**, 2530–2533.

53 D. T. Hog and M. Oestreich, *Eur. J. Org. Chem.*, 2009, **2009**, 5047–5056.

54 M. Mewald and M. Oestreich, *Chem.–Eur. J.*, 2012, **18**, 14079–14084.

55 D. J. Parks and W. E. Piers, *J. Am. Chem. Soc.*, 1996, **118**, 9440–9441.

56 D. J. Parks, J. M. Blackwell and W. E. Piers, *J. Org. Chem.*, 2000, **65**, 3090–3098.

57 P. Bach, A. Albright and K. K. Laali, *Eur. J. Org. Chem.*, 2009, **2009**, 1961–1966.

58 S. Rendler and M. Oestreich, *Angew. Chem., Int. Ed.*, 2008, **47**, 5997–6000.

59 R. Kannan, R. Chambenahalli, S. Kumar, A. Krishna, A. P. Andrews, E. D. Jemmis and A. Venugopal, *Chem. Commun.*, 2019, **55**, 14629–14632.

60 K. Sakata and H. Fujimoto, *J. Org. Chem.*, 2013, **78**, 12505–12512.

61 (*a*) W. E. Piers, A. J. V. Marwitz and L. G. Mercier, *Inorg. Chem.*, 2011, **50**, 12252–12262; (*b*) A. Y. Houghton, J. Hurmalainen, A. Mansikkamäki, W. E. Piers and H. M. Tuononen, *Nat. Chem.*, 2014, **6**, 983–988.

62 N. Asao, T. Sudo and Y. Yamamoto, *J. Org. Chem.*, 1996, **61**, 7654–7655.

63 (*a*) K. Revunova and G. I. Nikonov, *Dalton Trans.*, 2015, **44**, 840–866; (*b*) H.-J. Jung, Y. Cho, D. Kim and P. Mehrkhodavandi, *Catal. Sci. Technol.*, 2021, **11**, 62–91.

64 A. J. Blake, A. Cunningham, A. Ford, S. J. Teat and S. Woodward, *Chem.–Eur. J.*, 2000, **6**, 3586–3594.

65 (*a*) J. A. B. Abdalla, I. M. Riddlestone, R. Tirfoin and S. Aldridge, *Angew. Chem., Int. Ed.*, 2015, **54**, 5098–5102; (*b*) M. Saleh, D. R. Powell and R. J. Wehmschulte, *Organometallics*, 2017, **36**, 4810–4815; (*c*) A. Caise, J. Hicks, M. Ángeles Fuentes, J. M. Goicoechea and S. Aldridge, *Chem.–Eur. J.*, 2021, **27**, 2138–2148.

66 W. M. Haynes, *CRC Handbook of Chemistry and Physics*, CRC Press, London, 93rd edn, 2016.

67 (*a*) A. J. Chalk and J. F. Harrod, *J. Am. Chem. Soc.*, 1965, **87**, 16–21; (*b*) G. Giorgi, F. de Angelis, N. Re and A. Sgamellotti, *Future Gener. Comput. Syst.*, 2004, **20**, 781–791.

68 M. Rohde, L. O. Müller, D. Himmel, H. Scherer and I. Krossing, *Chem.–Eur. J.*, 2014, **20**, 1218–1222.

69 A. Martens, P. Weis, M. C. Krummer, M. Kreuzer, A. Meierhöfer, S. C. Meier, J. Bohnenberger, H. Scherer, I. Riddlestone and I. Krossing, *Chem. Sci.*, 2018, **9**, 7058–7068.

70 A. Schäfer, M. Reissmann, A. Schäfer, W. Saak, D. Haase and T. Müller, *Angew. Chem., Int. Ed.*, 2011, **50**, 12636–12638.

71 A. Schulz and A. Villinger, *Angew. Chem., Int. Ed.*, 2012, **51**, 4526–4528.

72 (*a*) C. Eaborn, P. D. Lickiss, S. T. Najim and W. A. Stańczyk, *J. Chem. Soc., Chem. Commun.*, 1987, 1461–1462; (*b*) N. Choi, P. D. Lickiss, M. McPartlin, P. C. Masangane and G. L. Veneziani, *Chem. Commun.*, 2005, 6023–6025; (*c*) N. Lühmann, H. Hirao, S. Shaik and T. Müller, *Organometallics*, 2011, **30**, 4087–4096; (*d*) K. Müther, P. Hrobárik, V. Hrobáriková, M. Kaupp and M. Oestreich, *Chem.–Eur. J.*, 2013, **19**, 16579–16594; (*e*) R. Labbow, F. Reiß, A. Schulz and A. Villinger, *Organometallics*, 2014, **33**, 3223–3226; (*f*) L. Albers, S. Rathjen, J. Baumgartner, C. Marschner and T. Müller, *J. Am. Chem. Soc.*, 2016, **138**, 6886–6892.

73 A. Schäfer, M. Reißmann, S. Jung, A. Schäfer, W. Saak, E. Brendler and T. Müller, *Organometallics*, 2013, **32**, 4713–4722.

74 K. Bläsing, R. Labbow, D. Michalik, F. Reiß, A. Schulz, A. Villinger and S. Walker, *Chem.–Eur. J.*, 2020, **26**, 1640–1652.

75 L. Omann, B. Pudasaini, E. Irran, H. F. T. Klare, M.-H. Baik and M. Oestreich, *Chem. Sci.*, 2018, **9**, 5600–5607.

76 J. Y.-C. Chen, A. A. Martí, N. J. Turro, K. Komatsu, Y. Murata and R. G. Lawler, *J. Phys. Chem. B*, 2010, **114**, 14689–14695.

77 A. Budanow, M. Bolte, M. Wagner and H.-W. Lerner, *Eur. J. Inorg. Chem.*, 2015, **2015**, 2524–2527.

78 (*a*) Z. Xie, J. Manning, R. W. Reed, R. Mathur, P. D. W. Boyd, A. Benesi and C. A. Reed, *J. Am. Chem. Soc.*, 1996, **118**, 2922–2928; (*b*) C. A. Reed, *Acc. Chem. Res.*, 1998, **31**, 325–332.

79 (*a*) L. Kloo, J. Rosdahl and M. J. Taylor, *Polyhedron*, 2002, **21**, 519–524; (*b*) F. Fetzer, C. Schrenk, N. Pollard, A. Adeagbo, A. Z. Clayborne and A. Schnepf, *Chem. Commun.*, 2021, **57**, 3551–3554.

80 N. G. Connelly and W. E. Geiger, *Chem. Rev.*, 1996, **96**, 877–910.

81 H. H. Anderson, *J. Am. Chem. Soc.*, 1958, **80**, 5083–5085.

82 N. Moitra, K. Kanamori, T. Shimada, K. Takeda, Y. H. Ikuhara, X. Gao and K. Nakanishi, *Adv. Funct. Mater.*, 2013, **23**, 2714–2722.

83 N. Moitra, K. Kanamori, Y. H. Ikuhara, X. Gao, Y. Zhu, G. Hasegawa, K. Takeda, T. Shimada and K. Nakanishi, *J. Mater. Chem. A*, 2014, **2**, 12535–12544.

84 M. Ohashi, R. Yaokawa, Y. Takatani and H. Nakano, *ChemNanoMat*, 2017, **3**, 534–537.

85 A. Sugie, T. Somete, K. Kanie, A. Muramatsu and A. Mori, *Chem. Commun.*, 2008, 3882–3884.

86 Ö. Dag, E. J. Henderson, W. Wang, J. E. Lofgreen, S. Petrov, P. M. Brodersen and G. A. Ozin, *J. Am. Chem. Soc.*, 2011, **133**, 17454–17462.
87 J. V. Crivello, *Silicon*, 2009, **1**, 111–124.
88 F. Yonehara, Y. Kido, H. Sugimoto, S. Morita and M. Yamaguchi, *J. Org. Chem.*, 2003, **68**, 6752–6759.
89 H. F. T. Klare and M. Oestreich, *Dalton Trans.*, 2010, **39**, 9176–9184.
90 H. F. T. Klare, L. Albers, L. Süsse, S. Keess, T. Müller and M. Oestreich, *Chem. Rev.*, 2021, **121**, 5889–5985.
91 (*a*) K. Hensen, T. Zengerly, P. Pickel and G. Klebe, *Angew. Chem., Int. Ed.*, 1983, **22**, 973–984; (*b*) G. K. S. Prakash, S. Keyaniyan, R. Aniszfeld, L. Heiliger, G. A. Olah, R. C. Stevens, H. K. Choi and R. Bau, *J. Am. Chem. Soc.*, 1987, **109**, 5123–5126; (*c*) J. B. Lambert, S. Zhang, C. L. Stern and J. C. Huffman, *Science*, 1993, **260**, 1917–1918.
92 (*a*) S. P. Hoffmann, T. Kato, F. S. Tham and C. A. Reed, *Chem. Commun.*, 2006, 767–769; (*b*) C. A. Reed, *Acc. Chem. Res.*, 2010, **43**, 121–128; (*c*) C. Bolli, J. Derendorf, C. Jenne, H. Scherer, C. P. Sindlinger and B. Wegener, *Chem.–Eur. J.*, 2014, **20**, 13783–13792.
93 S. J. Connelly, W. Kaminsky and D. M. Heinekey, *Organometallics*, 2013, **32**, 7478–7481.
94 M. Nava and C. A. Reed, *Organometallics*, 2011, **30**, 4798–4800.
95 J. B. Lambert and Y. Zhao, *J. Am. Chem. Soc.*, 1996, **118**, 7867–7868.
96 J. B. Lambert, Y. Zhao and H. Wu, *J. Org. Chem.*, 1999, **64**, 2729–2736.
97 A. Martens, M. Kreuzer, A. Ripp, M. Schneider, D. Himmel, H. Scherer and I. Krossing, *Chem. Sci.*, 2019, **10**, 2821–2829.
98 V. J. Scott, R. Çelenligil-Çetin and O. V. Ozerov, *J. Am. Chem. Soc.*, 2005, **127**, 2852–2853.
99 L. Süsse, J. Hermeke and M. Oestreich, *J. Am. Chem. Soc.*, 2016, **138**, 6940–6943.
100 I. Krossing, H. Brands, R. Feuerhake and S. Koenig, *J. Fluorine Chem.*, 2001, **112**, 83–90.
101 (*a*) P. D. Bartlett, F. E. Condon and A. Schneider, *J. Am. Chem. Soc.*, 1944, **66**, 1531–1539; (*b*) J. Y. Corey and R. West, *J. Am. Chem. Soc.*, 1963, **85**, 2430–2433; (*c*) J. Y. Corey, *J. Am. Chem. Soc.*, 1975, **97**, 3237–3238.
102 (*a*) R. A. McClelland, N. Banait and S. Steenken, *J. Am. Chem. Soc.*, 1986, **108**, 7023–7027; (*b*) V. R. Naidu, S. Ni and J. Franzén, *ChemCatChem*, 2015, **7**, 1896–1905.
103 J. S. Siegel, *Nat. Rev. Chem.*, 2020, **4**, 4–5.
104 C. Douvris and O. V. Ozerov, *Science*, 2008, **321**, 1188–1190.
105 D. O'Hagan, *Chem. Soc. Rev.*, 2008, **37**, 308–319.
106 C. B. Caputo and D. W. Stephan, *Organometallics*, 2012, **31**, 27–30.
107 M. H. Holthausen, M. Mehta and D. W. Stephan, *Angew. Chem., Int. Ed.*, 2014, **53**, 6538–6541.
108 J. H. W. LaFortune, T. C. Johnstone, M. Pérez, D. Winkelhaus, V. Podgorny and D. W. Stephan, *Dalton Trans.*, 2016, **45**, 18156–18162.
109 S. Postle, V. Podgorny and D. W. Stephan, *Dalton Trans.*, 2016, **45**, 14651–14657.
110 K. M. Szkop and D. W. Stephan, *Dalton Trans.*, 2017, **46**, 3921–3928.
111 R. Maskey, M. Schädler, C. Legler and L. Greb, *Angew. Chem., Int. Ed.*, 2018, **57**, 1717–1720.
112 S. S. Chitnis, F. Krischer and D. W. Stephan, *Chem.–Eur. J.*, 2018, **24**, 6543–6546.
113 D. B. Culver and M. P. Conley, *Angew. Chem., Int. Ed.*, 2018, **57**, 14902–14905.
114 D. Hartmann, M. Schädler and L. Greb, *Chem. Sci.*, 2019, **10**, 7379–7388.
115 N. Kramer, H. Wadepohl and L. Greb, *Chem. Commun.*, 2019, **55**, 7764–7767.
116 M. Mehta and J. M. Goicoechea, *Angew. Chem., Int. Ed.*, 2020, **59**, 2715–2719.
117 A. Hermannsdorfer and M. Driess, *Angew. Chem., Int. Ed.*, 2020, **59**, 23132–23136.
118 K. I. Burton, I. Elser, A. E. Waked, T. Wagener, R. J. Andrews, F. Glorius and D. W. Stephan, *Chem.–Eur. J.*, 2021, **27**, 11730–11737.
119 C. Douvris, C. M. Nagaraja, C.-H. Chen, B. M. Foxman and O. V. Ozerov, *J. Am. Chem. Soc.*, 2010, **132**, 4946–4953.
120 (*a*) G. Baddeley, *Q. Rev., Chem. Soc.*, 1954, **8**, 355–379; (*b*) V. Polito, C. S. Hamann and I. J. Rhile, *J. Chem. Educ.*, 2010, **87**, 969–970.
121 D. M. Lemal, *J. Org. Chem.*, 2004, **69**, 1–11.
122 (*a*) P. J. Malinowski, T. Jaroń, M. Domańska, J. M. Slattery, M. Schmitt and I. Krossing, *Dalton Trans.*, 2020, **49**, 7766–7773; (*b*) In *Experiments in Green and Sustainable Chemistry*, I. Raabe, A. Reisinger, I. Krossing, H. W. Roesky and D. K. Kennepohl, Wiley-VCH, Weinheim, 2009, pp. 131–144.
123 Can be purchased under https://www.iolitec.de.
124 M. Schorpp, R. Tamim and I. Krossing, *Dalton Trans.*, 2021, **50**, 15103–15110.